

# IMPROVING TECHNOLOGY FOR MANUFACTURING CASTING CASE OF TRUCK CLUTCH RELEASE CYLINDER

**Dmitriy Demin**

«Scientific Route» OÜ, Tallinn, Estonia

E-mail: info@eu-jr.eu

ORCID: <https://orcid.org/0000-0002-7946-3651>

## ARTICLE INFO

### Article history:

Received date 07.03.2023

Accepted date 18.04.2023

Published date 30.04.2023

### Section:

Metallurgy

## DOI

10.21303/2313-8416.2023.003194

## KEY WORDS

iron casting  
body castings  
clutch cylinder body  
duplex melt process  
alloying  
modification

## ABSTRACT

**The object of research:** manufacturing technology of body castings for trucks using the example of a clutch release cylinder body made of gray cast iron with flake graphite EN-GJL-200.

**Investigated problem:** finding ways to reduce the weight and size characteristics of cast parts.

**The main scientific results:** a mathematical model has been developed that has made it possible to determine the optimal compositions of alloying Cr/Ni – Cu/Ti complexes that ensure an increase in the grade of cast iron by increasing the tensile strength at elevated carbon contents. This makes it possible in the future to reduce the thickness of the walls of the castings, achieving a reduction in their weight and size characteristics

**The area of practical use of the results of the study:** automotive industry in terms of technology for manufacturing cast parts for trucks

**Innovative technological product:** improved technology for manufacturing the clutch release cylinder body due to optimization of melt technology and out-of-furnace processing allows for targeted selection of melt processing modes, ensuring an increase in the strength characteristics of cast iron for cast body parts, thereby moving from the EN-GJL-200 cast iron grade to the EN-GJL-250 and EN-GJL-300 grades.

**The scope of the innovative technological product:** foundries of engineering enterprises, in particular those producing trucks, in which iron castings are produced

© The Author(s) 2023. This is an open access article under the Creative Commons CC BY license

## 1. Introduction

### 1.1. The object of research

The object of research is the technology of manufacturing body castings for trucks using the example of a clutch release cylinder body made of gray cast iron with flake graphite EN-GJL-200.

### 1.2. Problem description

Reducing the weight and size characteristics of machine parts and mechanisms is a complex design and technological task that must be solved at many stages of machine manufacturing. First of all, such tasks are related to the need to search for technological solutions at the stage of procurement production. Considering the fact that most machine parts, in particular cars, are cast, the problem comes down to developing solutions to improve the mechanical characteristics of alloys at the stage of their manufacture. This means that, first of all, it is necessary to develop rational or optimal technological regimes for melt and out-of-furnace processing, based on optimizing the compositions and structure of the alloys. In combination with minimizing allowances for machining, this will make it possible to reduce the weight and size characteristics of machine parts while maintaining their operational reliability.

### 1.3. Suggested solution to the problem

Body castings for the manufacture of machine-building parts, in particular for parts of trucks, are manufactured mainly in serial and mass production in one-time sand molds. At each section of the technological process, they try to find rational and, if possible, optimal solutions to maximize the quality of the product of this section, minimize resource and energy costs, or maximize productivity. The solutions found, which are the best according to the selected criteria, can be incorporated into production management systems, which include, among other things, the possibility of its automation.

There are known solutions related to areas of cast iron melt in cupola furnaces, based on the search for ways to intensify the process [1, 2], its adequate technological description [3], the choice

of a rational layout of technical means and the structure of the melt process control system [4, 5], the search for ways increasing its environmental safety [6]. Conceptual solutions for the synthesis of optimal control of cupola melt are presented in [7]. According to this work, the optimal control of the melt temperature regime (**Fig. 1**) can be found on the basis of Pontryagin’s maximum principle, solving two problems: constructing an optimal law for regulating the level of the idle shell height and synthesizing optimal control of air flow.

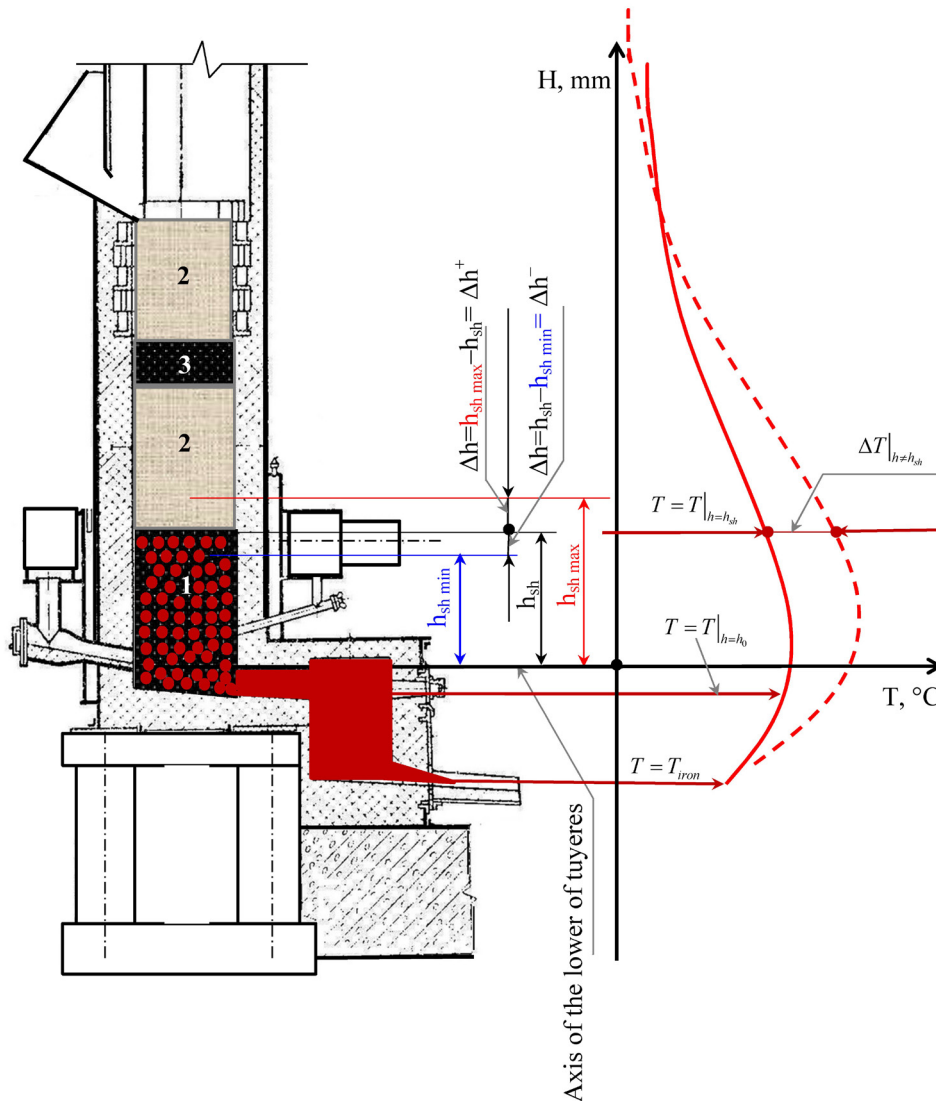


**Fig. 1.** Visualization of the cupola temperature profile by loading zones [7]: 1 – idle charge; 2 – metal charge; 3 – fuel charge;  $H$  – horizon level along the cupola furnace height,  $h$  – current coordinate along the cupola furnace height,  $h_{sh}$  – horizon along the cupola furnace height, corresponding to the position of the upper level of the idle charge,  $h_{sh\ max}$  – maximum horizon along the cupola height, corresponding to the minimum position of the upper level of the idle charge,  $h_{sh\ min}$  – the minimum horizon along the height of the cupola, corresponding to the maximum position of the upper level of the idle charge,  $\Delta h^+$  – the positive deviation of the upper level of the idle charge along the horizon,  $\Delta h^-$  – the negative deviation of the upper level of the idle charge along the horizon,  $T$  – the temperature in the cupola,  $T_{iron}$  – the temperature of the cast iron when discharged from cupola furnaces

In the first case, the control law has the form (1), and the phase trajectory has the form (2):

$$u_{1opt} = u_{10} \operatorname{sgn} \left[ \frac{1}{2u_0} (x_1 - q)^2 \operatorname{sgn}(q - x_1) - x_2 \right], \tag{1}$$

$$x_2 = \frac{1}{2u_1}(x_1 - q)^2 + x_2^{(0)} - \frac{1}{2u_1}(x_1^{(0)} - q)^2, \quad (2)$$

where  $x_1 = \Delta Q_{c1}$  – the change in coke consumption loaded into the cupola,  $x_2 = F\Delta h_{sh}$  – the change in the volume of the fuel charge with increasing consumption  $Q_{c2}$ ,  $q = \Delta Q_{c2}$  – the change in coke consumption due to the combustion process,  $(x_1^{(0)}, x_2^{(0)})$  – the initial state of the system,  $u_1 = kU_1$  – control proportional to voltage, applied to the electric motor, and the voltage value  $U$  is limited by the condition  $-U_{10} \leq U_1 \leq U_{10}$ ,  $k$  – an integral coefficient that takes into account the influence of the characteristics of a particular electric drive, and the phase trajectory (2) when applying control (1) can be obtained by solving the system of equations (3), based on the mathematical model of the process changes in the upper level of idle charges of the form (4):

$$\begin{cases} \frac{dx_1}{dt} = u_1, \\ \frac{dx_2}{dt} = x_1 - q, \end{cases} \quad (3)$$

$$F \frac{dh_{sh}}{dt} = Q_{c1} - Q_{c2}, \quad (4)$$

where  $F$  – the clear area of the cupola,  $Q_{c1}$  – the consumption of coke loaded into the cupola,  $Q_{c2}$  – the consumption of coke due to the combustion process, and the relationship between  $Q_{c1}$  and control is described by the equation

$$\frac{dQ_{c1}}{dt} = kU. \quad (5)$$

An increase in flow rate  $Q_{c2}$  causes the upper level of the idle ear to drop from the initial height by the amount  $\Delta h = h_{sh} - h_{sh \min} = \Delta h$ . This change is perceived by the control system, which loads the required portion of the fuel charge, which compensates for the consumption of coke  $Q_{c2}$ .

In the second case, the synthesis of optimal air flow control is carried out by implementing the algorithm presented in **Fig. 2**.

Optimal control of the implementation of the algorithm shown in **Fig. 2**, allows to control the temperature regime of cupola melt, ensuring the fulfillment of the criterion  $T_{iron} \rightarrow T_{iron \max}$  for the level of the height of the idle charge, maintained by the level controller, respectively (1).

The result of optimal control is maintaining a given temperature profile and returning it to a given position in the shortest possible time through the combined influence of the temperature regime: changing the amount of coke in the idle charge ( $V_c$ ) – control action  $u_1$ , and changing the flow rate of blown air ( $Q$ ) – control action  $u_2$  (**Fig. 3**).

However, the temperature regime is not the only factor influencing the chemical composition of cast iron when it is released from the cupola. An important role is played by the composition of the charge, which may not be stable. In addition, the composition of the charge may not be controlled at all. A generalization of the results of retrospective industrial studies [8] shows that reducing the uncertainty in assessing the chemical composition of cupola melt iron with an uncontrolled charge can be achieved if a certain ratio in the loading of charge components that introduce uncertainty is maintained. Among them are foundry and pig iron and scrap. **Table 1** shows typical charge compositions ( $i$  is an index characterizing the number of the charge component), and **Table 2** shows the chemical compositions and properties of cast iron smelted using these charge compositions ( $j$  is an index identifying an element of the chemical composition).

**Table 3** presents generalized data on the content of chemical elements in the composition of cast iron  $m_a(f_{ij})$  and their deviations  $S(f_{ij})$  in cast iron.

The permissible fields of deviations of values  $f_{ij}$  for standard grades of cast iron, based on ensuring the specified values of the generalized quality indicator, including hardness, tensile strength, carbon, silicon and phosphorus content in cast iron, correspond to those given in **Tables 4, 5**.

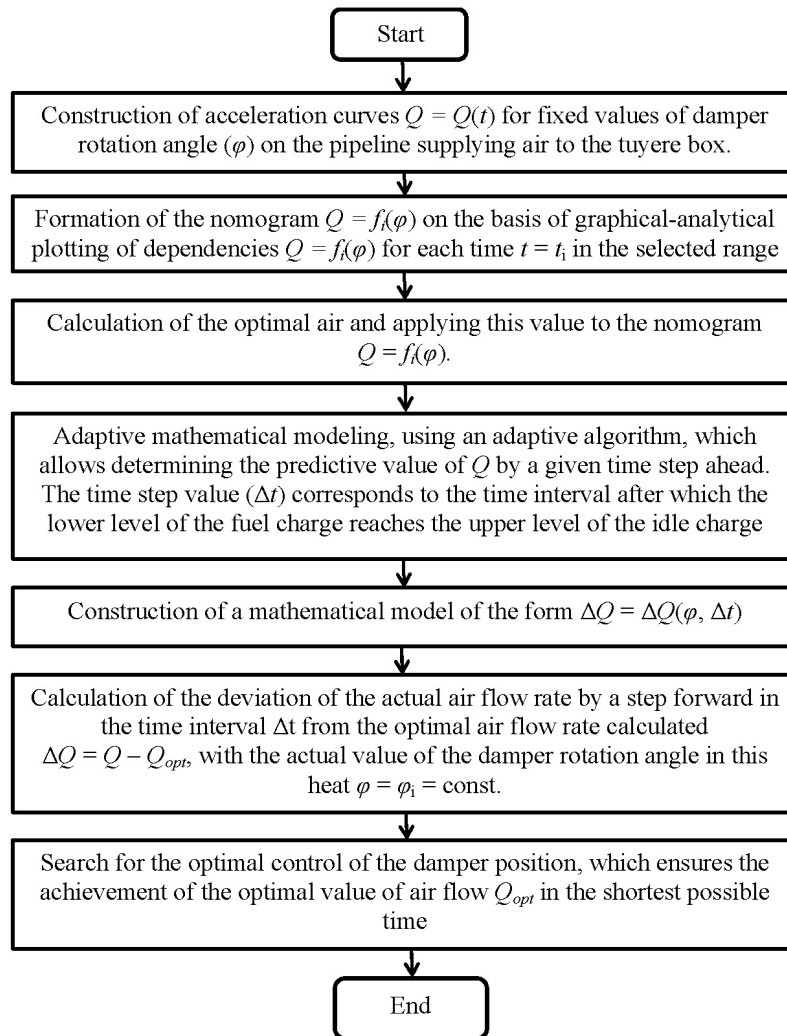


Fig. 2. Synthesis algorithm for optimal air flow control (built on the basis of the description given in [7])

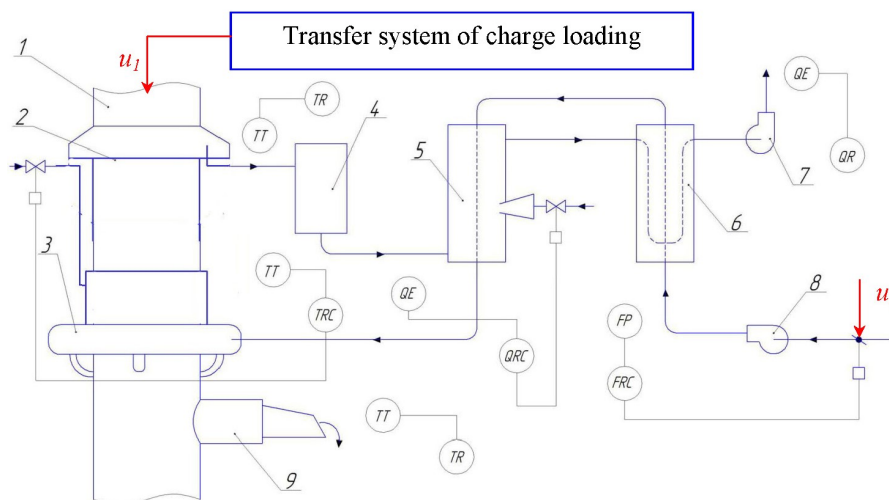


Fig. 3. Simplified scheme for controlling the cupola melt process [7]: 1 – cupola; 2 – spark arrester; 3 – tuyere belt; 4 – wet cleaner; 5 – radiation recuperator; 6 – convective recuperator; 7 – smoke exhauster; 8 – fan; 9 – storage tank

**Table 1**

Charge compositions, chemical compositions and properties of cast iron of different grades

Charge, composition and properties of cast iron	Charge composition, $g_{ik}$ , $k=1, \dots, 10$									
	1	2	3	4	5	6	7	8	9	10
Cast iron ( $i=1$ )	40.2	30	30.1	25.1	10	9.8	4.9	–	–	–
Pig iron ( $i=2$ )	–	9.7	12.2	18.1	24.2	31	35.2	39.8	45	39.6
Return ( $i=3$ )	42.5	37.4	40.1	38	38.7	40	39.3	40.3	35.3	26.8
Scrap ( $i=4$ )	7.6	11.2	10.2	10.1	10.2	10.1	9.8	10	9.8	12.8
Ferrolloys ( $i=5$ )	1.1	3.5	4.1	4.7	6.8	5.1	6.9	6.4	6	6.9

**Table 2**

Chemical compositions and properties of cast iron smelted on the charges given in Table 1

Chemical composition of cast iron, wt. %										
C ( $j=1$ )	3.27	3.22	3.17	3.33	3.26	3.15	3.29	3.24	3.28	3.40
Si ( $j=2$ )	2.77	2.17	2.27	2.45	2.53	2.31	2.41	2.56	2.40	2.27
P ( $j=3$ )	0.19	0.19	0.18	0.17	0.18	0.18	0.18	0.18	0.18	0.18
Mechanical properties										
$\sigma_B$ , MPa	277	286	260	273	273	285	281	264	251	235
HB	235	244	236	223	238	240	240	239	246	228
$\Sigma_f$ , MPa	492	537	500	511	487	513	516	514	512	475

**Table 3**

 Generalized data on the values of  $f_{ij}$  and their deviations in cast irons

Cast iron grade	Parameters of sample functions $f_{ij}$ , %					
	$f_{11}$		$f_{13}$		$f_{12}$	
	$m_a(f_{11})$	$S(f_{11})$	$m_a(f_{13})$	$S(f_{13})$	$m_a(f_{12})$	$S(f_{12})$
L1	3.75	0.083	3.4	0.066	0.71	0.066
L2	3.85	0.083	3.0	0.066	0.71	0.066
L3	3.95	0.083	2.6	0.066	0.71	0.066
L4	4.05	0.083	2.2	0.066	0.71	0.066
L5	4.15	0.083	1.8	0.066	0.71	0.066
L6	4.25	0.083	1.4	0.066	0.71	0.066
L7	4.35	0.083	1.0	0.066	0.71	0.066

**Table 4**

 Allowable fields of deviations in  $f_{i1}$  value

Cast iron grade according to GOST 1412-85	$(f_{i1}^{\min}; f_{i1}^{\max})$		$\delta_{f_{i1}}$	
	$i=2$	$i=1$	$i=2$	$i=1$
	EN-GJL-150		4.16–4.52	
EN-GJL-200	4–4.5	3.36–3.72	$\pm 0.25$	$\pm 0.18$
EN-GJL-250		3.36–3.57		$\pm 0.105$

**Table 5**

 Allowable fields of deviations in  $f_{i3}$  value

Cast iron grade according to GOST 1412-85	$(f_{i3}^{\min}; f_{i3}^{\max})$		$\delta_{f_{i3}}$	
	$i=2$	$i=1$	$i=2$	$i=1$
	EN-GJL-150		0.70–1.24	
EN-GJL-200	0.5–1.3	0.98–1.36	$\pm 0.4$	$\pm 0.19$
EN-GJL-250		0.98–1.36		$\pm 0.19$

Consequently, in order to increase the grade of cast iron and the selected generalized quality indicator, the consumption rate of pig iron should decrease. At the same time, the share of silicon introduced with return, scrap and ferroalloys decreases. Statistical processing of data from industrial melts has shown that in practical conditions, the selection of charge components should be carried out in such a way that the amount of cast iron falls into the region  $(35.5 - 0.883g_{2k}) \leq g_{1k} \leq (40.46 - 0.883g_{2k})$ . Maintaining this condition minimizes the uncertainty in assessing the influence of the quality of the charge on the formation of the chemical composition of the cast iron produced from the cupola. However, the accuracy and regularity of loading the cupola should be monitored.

Conceptual solutions for managing loading processes are presented in [9]. The solutions proposed in it are focused on regulating the temperature and carbon content of cast iron. Thus, it is noted that the parameter that determines the need to regulate the temperature is the difference in the level of the idle charge. If it is insufficient, then the temperature of the cast iron drops, although the speed of the melt front increases. Therefore, regulation must be carried out by supplying additional working charge. **Fig. 4–6** shows a demonstration of the principle of temperature control.

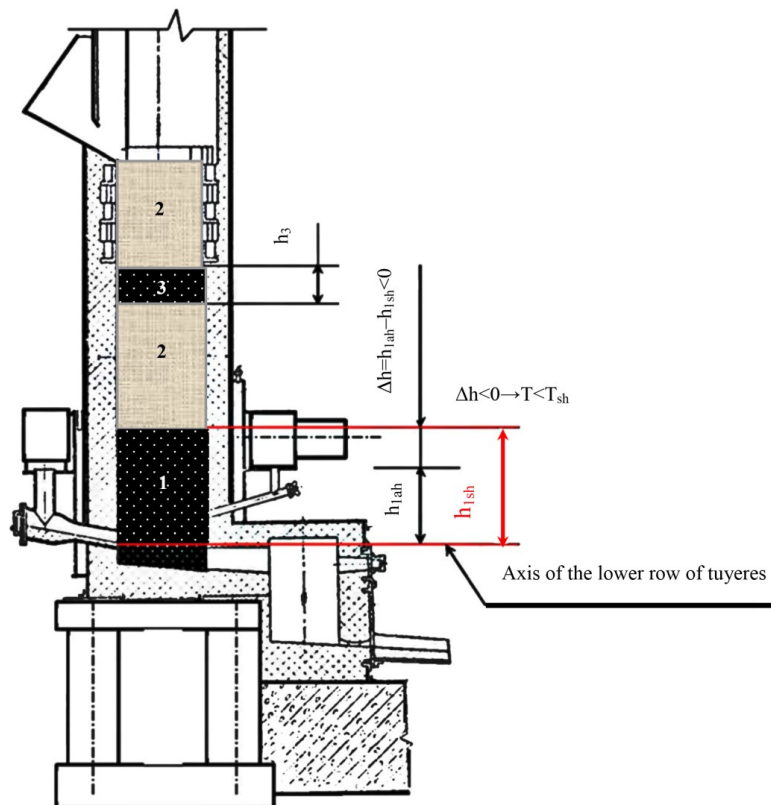


**Fig. 4.** Temperature control conditions [9]: 1 – idle charge; 2 – metal charge; 3 – working fuel charge;  $\Delta h$  – height difference of the idle charge, mm;  $T$  – actual (recorded) temperature of cast iron;  $T_{sh}$  – set temperature of cast iron,  $h_3$  – height of the working fuel charge introduced into the cupola to adjust the temperature, determined from the  $V_{coke}$  value with the existing cupola diameter in the light;  $V_{coke}$  – coke volume idle charge

If the level of idle charge is higher than necessary, then the parameter determining the need for regulation is the cupola productivity. Therefore, performance control should be performed by supplying an additional metal charge. **Fig. 7–9** show a demonstration of the control principle.

Technical implementation options are presented in **Fig. 10, 11**.

The presented technical implementation options reflect the operating principle of the «charge loading system» block of the structural diagram of the temperature and cupola capacity controller shown in **Fig. 5, 8**.

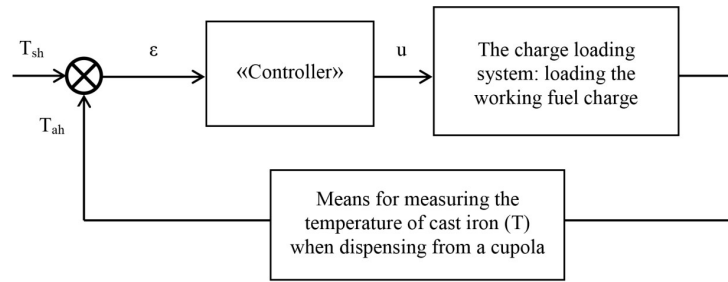


Fig. 5. The block diagram of the temperature controller [9]

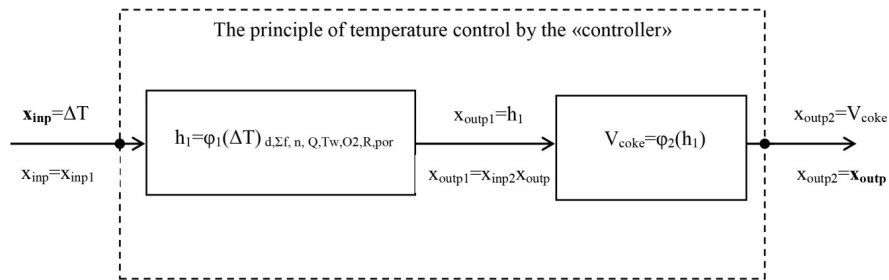


Fig. 6. The principle of temperature regulation [9]:

$h_1$  – idle charge level, mm;  $\varphi_1(\Delta T)_{d,\Sigma f,n,Q,Tw,O_2,Rpor}$  – temperature difference function of cast iron at the actual design parameters of the cupola and the actual technological melt conditions:  
 $d$  – diameter of the cupola in the light;  $\Sigma f$  – total sectional area of the tuyeres;  
 $n$  – number of rows of tuyeres;  $W$  – amount of air supplied to the cupola;  $Tw$  – temperature of the air supplied to the cupola;  $O_2$  – oxygen concentration in the air supplied to the cupola;  
 $Rpor$  – the porosity of an idle charge

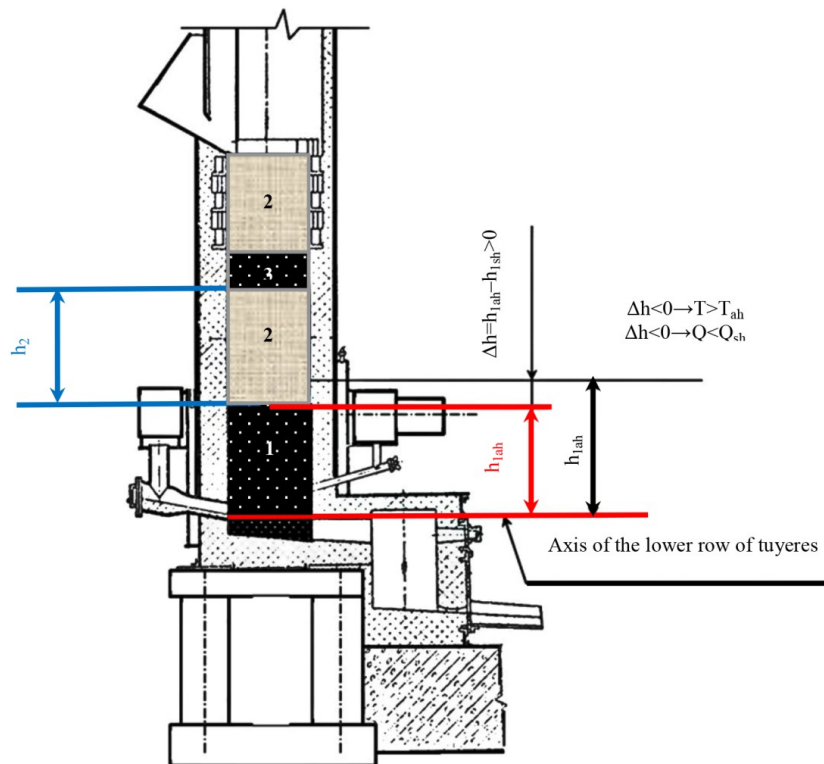


Fig. 7. Conditions for productivity control: 1 – idle charge; 2 – metal charge; 3 – working fuel charge [9].  $h_2$  – height of the metal spike

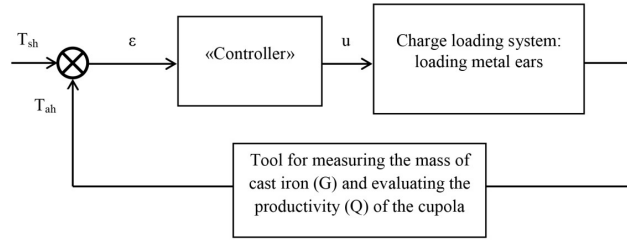


Fig. 8. Block diagram of the cupola performance controller [9]

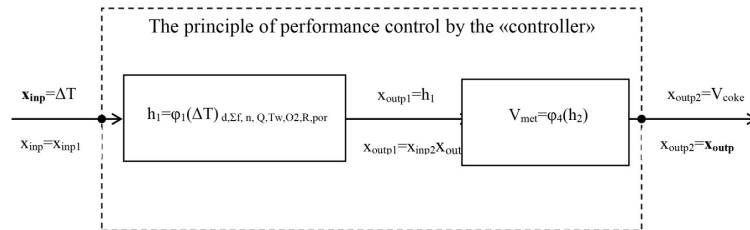


Fig. 9. The principle of controlling the cupola productivity [9]:  $V_{met}$  – volume of the furnace charge in a metal charge

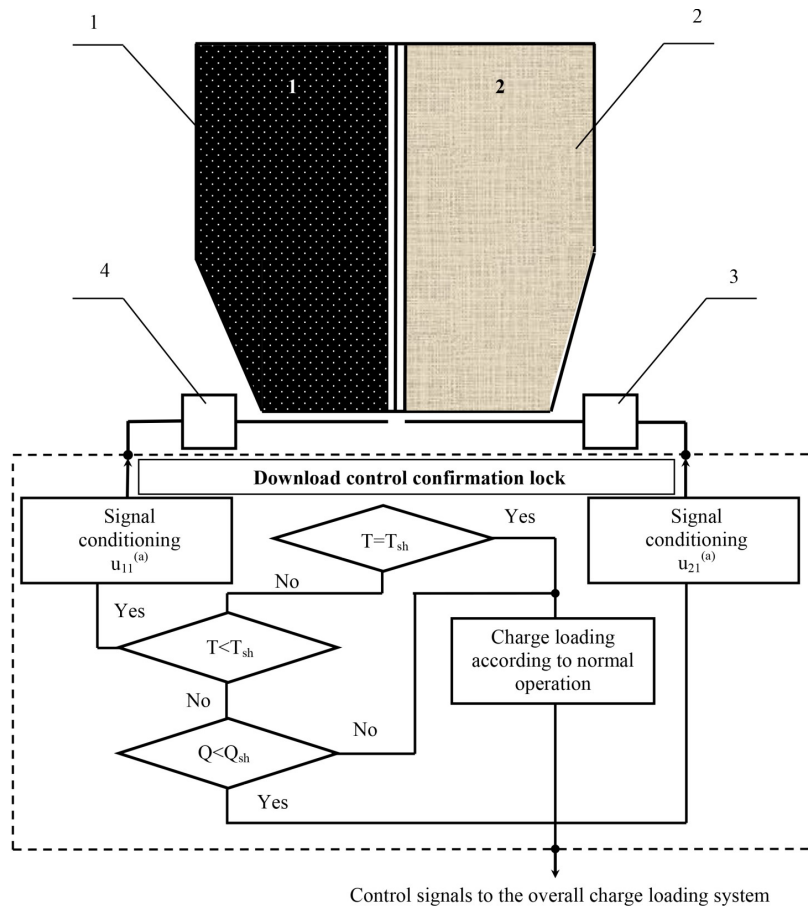
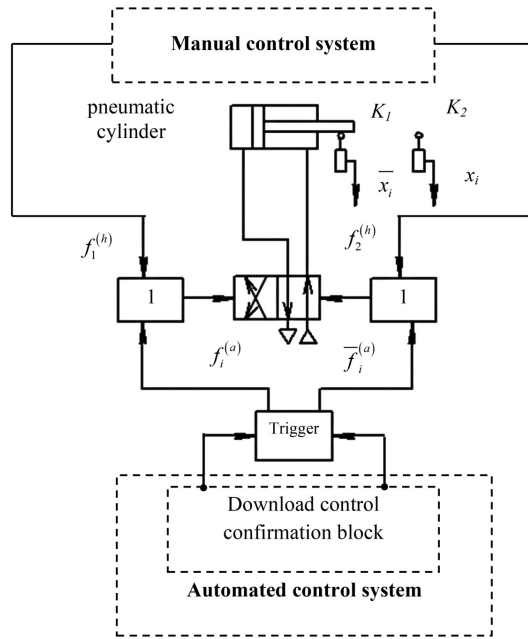


Fig. 10. The block diagram of the part of the loading control system, including regulation of the temperature and productivity of the cupola by supplying a working fuel and metal charge: 1 – hopper with coke; 2 – hopper with a metal charge; 3 – actuator of the loading system of the metal charges; 4 – actuator loading system of the working fuel charge [9];  $u_{11}^{(a)}$  – including the signal of the drive of the gate of the hopper with coke coming from the automated control system;  $u_{21}^{(a)}$  – the switching signal of the hopper gate drive with a metal charge coming from the automated control system (Fig. 11)





**Fig. 11.** Element of the control system of the gate valves of the hopper dampers [9].  $K_1, K_2$  – limit switches near and far, respectively;  $f_1^{(h)}, f_2^{(h)}$  – control signals coming to the solenoids of the distributors from the manual control system;  $f_i^{(a)}, \bar{f}_i^{(a)}$  – control signals coming to the solenoids of the valves from the trigger from the automated control system;  $u_{i1}^{(a)}, u_{i0}^{(a)}$  – control signals coming from the automated control system to the switching inputs of the trigger

Considering that the chemical composition of the cast iron produced from the cupola is unstable, its temperature is not high enough and it contains high levels of carbon and sulfur, a secondary unit is used. Typically, such a unit is an induction furnace, in which a high-quality process of temperature regulation is possible [10, 11] and control of the process of forming a given composition and properties of cast iron, taking into account performance requirements [12].

If there are no induction furnaces in the workshop, but there are electric arc furnaces, such furnaces can become a secondary unit. However, in this case, it is necessary to take a comprehensive approach to optimization issues, considering electric arc furnaces from the position of complex energy technological systems [13, 14], the efficiency of which as a secondary unit intended for thermal and temporary processing of molten cast iron in mixer mode is very low, reaching approximately 25 %.

To form the final properties of the alloy, its chemical composition is optimized [15], allowing the composition of the charge to be selected, and optimal or rational modification modes are selected [16]. It is possible to use technological methods of combining modification with alloying [17–19], which results in an increase in the mechanical properties of cast iron [20, 21]. Such operations can be carried out at the stage of out-of-furnace processing of the alloy [22], and the choice of specific modes is carried out on the basis of mathematical models of the “composition - properties” type [23]. Such optimal or rational solutions in the technology of melt and after-furnace processing form the metallurgical component of the quality of castings. The second part of quality is formed by technological and technical solutions for the production of casting molds. In this regard, it is necessary to mention studies devoted to the improvement of technological molding processes aimed at improving the operation of shake-press [24, 25] and pressing [26] machines.

Thus, in [24, 25] regression equations are presented that describe the process of mixture compaction in the variables “number of table impacts ( $x_1$ ) – compressed air pressure ( $x_2$ )”, which determine the coefficient of recovery upon impact of the mixture  $y_1$  and the height of reflection of the mixture  $y_2$ :

$$y_1 = 0.221 + 0.12x_1 + 0.055x_2 \tag{6}$$

$$y_2 = 8.803 + 3.9x_1 + 3.217x_2. \tag{7}$$

This allows to rationally control the compaction process, achieving not only a given density, but also reducing energy costs, and can be used to improve the control system of molding machines.

In [26], a method is proposed that does not require measuring the forces in the mixture compaction system by pressing, but allows one to obtain the dynamic characteristics of the pressing process based on an adaptive approach to determining the technological force. It is shown that the dynamic characteristics of the compaction process can be assessed directly in the industrial process, without measuring the forces acting in the system during bottom pressing. This can be done regardless of whether the drive is pneumatic or hydraulic and provides the ability to control the quality of the molds produced.

The result of the application of optimal or rational solutions in terms of molding is the formation of the quality of castings in terms of geometry and dimensional accuracy [27].

It should be noted that optimization of melt and mold manufacturing technology alone is not enough, given the productivity criterion, which is very important for production. Therefore, it is necessary to solve the problem of maximum consistency in the operation of the melt, mold assembly and pouring sections, which is possible by modeling this system as a queuing system, for example, as presented in [28]. In particular, it is important to coordinate the operation of holding furnaces, which can be electric mixers, acting as a secondary unit of the duplex melt process, and providing the pouring section of the casting conveyor with the required amount of alloy of a given quality in terms of chemical composition and temperature. If castings are subject to special requirements dictated by operational features, the task of obtaining high-quality castings becomes more complicated, since additional requirements may be imposed. For example, for the clutch cylinder housing of trucks, which is under high internal pressure, the requirement for tightness is especially important. It can be ensured by the formation of a microstructure in cast iron with a minimum graphite size. This ensures an increase in intergraphite layers in the metal matrix, preventing leakage due to the destruction of the matrix in the intergraphite partitions under internal pressure [29].

Thus, the proposed solution to the problem associated with the need to improve the technology for manufacturing body castings such as clutch cylinders for trucks could be:

- melt by duplex process;
- modification combined with alloying, ensuring maximum strength characteristics of the alloy and microstructure with minimal graphite sizes;
- rational modes of manufacturing molds;
- design and technological solutions aimed at reducing weight and size characteristics while maintaining the same mechanical properties.

## 2. Materials and Methods

### 2.1. Melt

Melt was carried out using a cupola-electric arc furnace duplex process (**Fig. 12**).

The melt was carried out in a site equipped with two cupola furnaces with a capacity of 5 t/h each, operating alternately.

The technical characteristics of the cupola are given in **Table 6**.

The process of loading and launching the cupola for melt is schematically represented by the algorithm in **Fig. 13**. The full cycle of operations is carried out in accordance with the melt instructions approved by the enterprise, in compliance with all safety standards.

Liquid cast iron from a cupola is fed to a mixer (**Fig. 1**), which is used as a ДЧМ-10 electric arc furnace with a volume of 10 tons. Thermal treatment of the melt is carried out in it, with the aim of bringing the cast iron temperature to a predetermined temperature (1370–1400 °C) and bringing the chemical composition to the specified, in accordance with the technical conditions for cast iron. The chemical composition of cupola iron cast into the mixer should correspond to the following: C=3.2–3.5 %, Si=1.5–1.8 %, Mn=0.2–0.6 %, S=0.05–0.12 %, P no more than 0.2 %, Cr=0.3–0.45 %, Ni=0.11–0.13 %, Cu=0.1–0.4 %, Ti=0.03–0.08 %. In the mixer, overheating and fine-tuning according to the chemical composition according to the silicon content to 2.3–2.5 %, manganese to 0.6–0.8 % are carried out.

Technical characteristics of the electric furnace-mixer DChM-10 are given in **Table 7**.

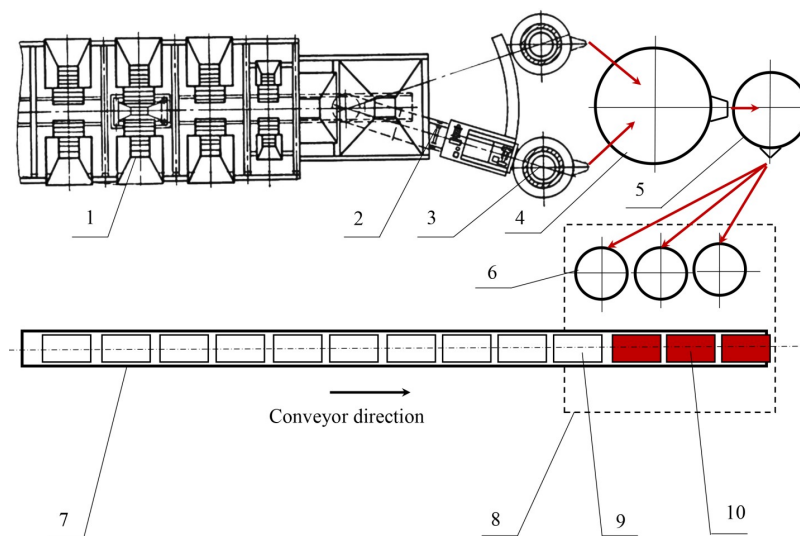


**Fig. 12.** «Cupola – electric arc furnace» duplex process scheme [9]: 1 – transfer system of charge loading; 2 – skip hoist; 3 – cupola; 4 – electric arc furnace (mixer); 5 – transfer bucket; 6 – casting buckets; 7 – casting conveyor; 8 – filling area; 9 – casting molds, ready for filling; 10 – filling forms

**Table 6**

Technical characteristics of the cupola

No.	Name	Dimension	Characteristic
1	Performance	t/h	5
2	Download method	–	skip lift
3	Diameter in the light	mm	900
4	Cross-sectional area	mm <sup>2</sup>	0.636
5	Useful height (from the axis of the lower row of tuyeres to the level of the filling window)	mm	4234
6	The number of the I row tuyeres	–	6
7	The number of the II row tuyeres	–	6
8	The number of the III row tuyeres	–	6
9	I row tuyere size	mm×mm	200×125
10	II row tuyere size	mm×mm	70×50
11	III row tuyere size	mm×mm	70×50
12	Receiver diameter	mm	820
13	Working capacity of a receiver	m <sup>3</sup>	0.283
14	Height from the hearth to the slag tap hole of the receiver	mm	450
15	Height from the hearth to the axis of the I row tuyeres	mm	400
16	Diameter of the slag tap hole	mm	50
17	Diameter of metal tap holes	mm	25
18	Number of metal tap holes	–	2
19	Transition window section	mm×mm	120×90
20	The mass of the loaded metal charges	kg	500
21	The mass of idle charges	kg	900–930
22	The height of the idle charge above the upper edge of the III row of tuyeres	mm	550–600
23	Air pressure in the tuyere box	mm wc	600–650
24	Fan type	–	A-72-2 No. 725766
25	Fan aperture diameter	mm	220

The melt is released from the cupola into the electric arc furnace (mixer) in portions (Fig. 14).

The process control diagram of the «cupola – mixer» technological system, focused on fulfilling the requirements is shown in Fig. 15.

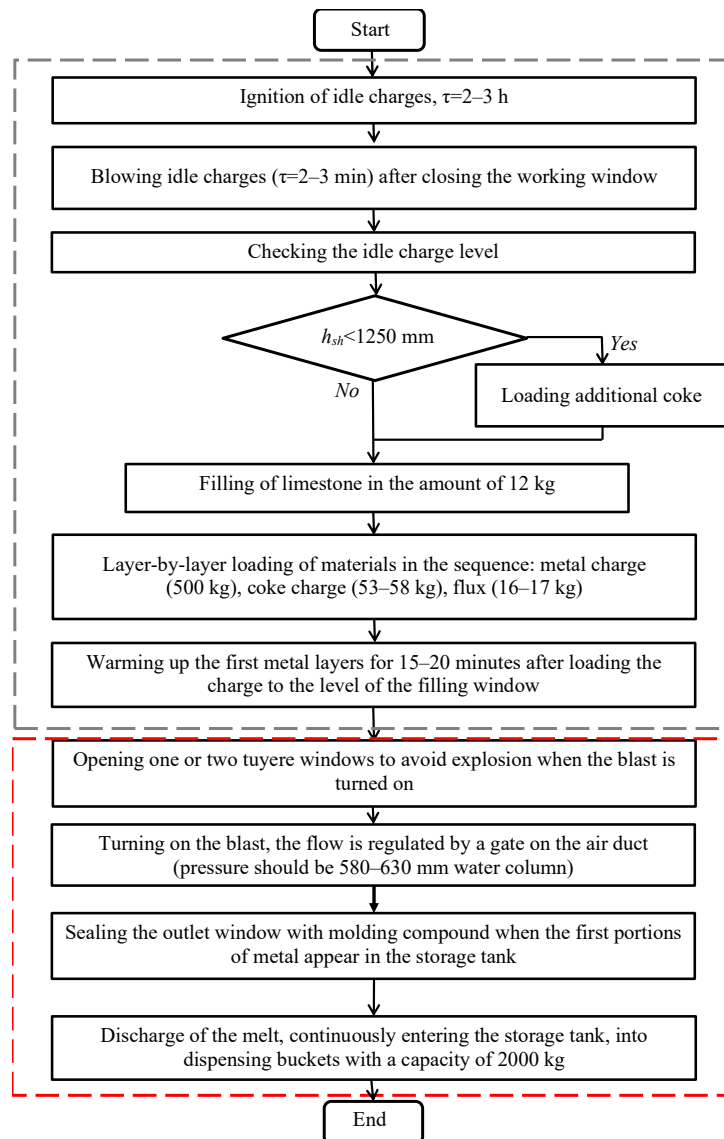


**Fig. 13.** Algorithm schematically describing the process of loading and launching a cupola furnace for melt. Constructed based on the description given in [9]:  
 □ □ □ – stage of preparation before melt; □ □ □ – stage of melt

In the mixer, the melt is overheated to a predetermined temperature of 1370–1400 °C and the chemical composition is brought to the desired one.

Correction of the chemical composition is carried out by introducing additives, depending on the element of the chemical composition, having deviations from the given content, falling outside the tolerance field. The introduction of additives is a control action with the aim of transferring the content of an element of chemical composition into the tolerance field. Such control actions are shown in **Tables 8, 9**.

The refinement of molten iron to a predetermined chemical composition for manganese (0.6–0.8) % is carried out in the ladle with an additive on the bottom of the ladle, crushed to a fraction of 1–10 mm, of dried 70 % ferromanganese blast furnace.

The content in silicon cast iron is adjusted by adding 25 % ferrosilicon to the mixer.

From the mixer, cast iron is delivered to the pouring section of the foundry conveyor, where disposable sand molds collected for pouring are received. The half-forms were made on shaking-press machines with additional pressing with rotation of the half-forms – for the production of lower half-forms and with additional pressing without turning the half-forms – for the production of upper half-forms (**Fig. 16**)

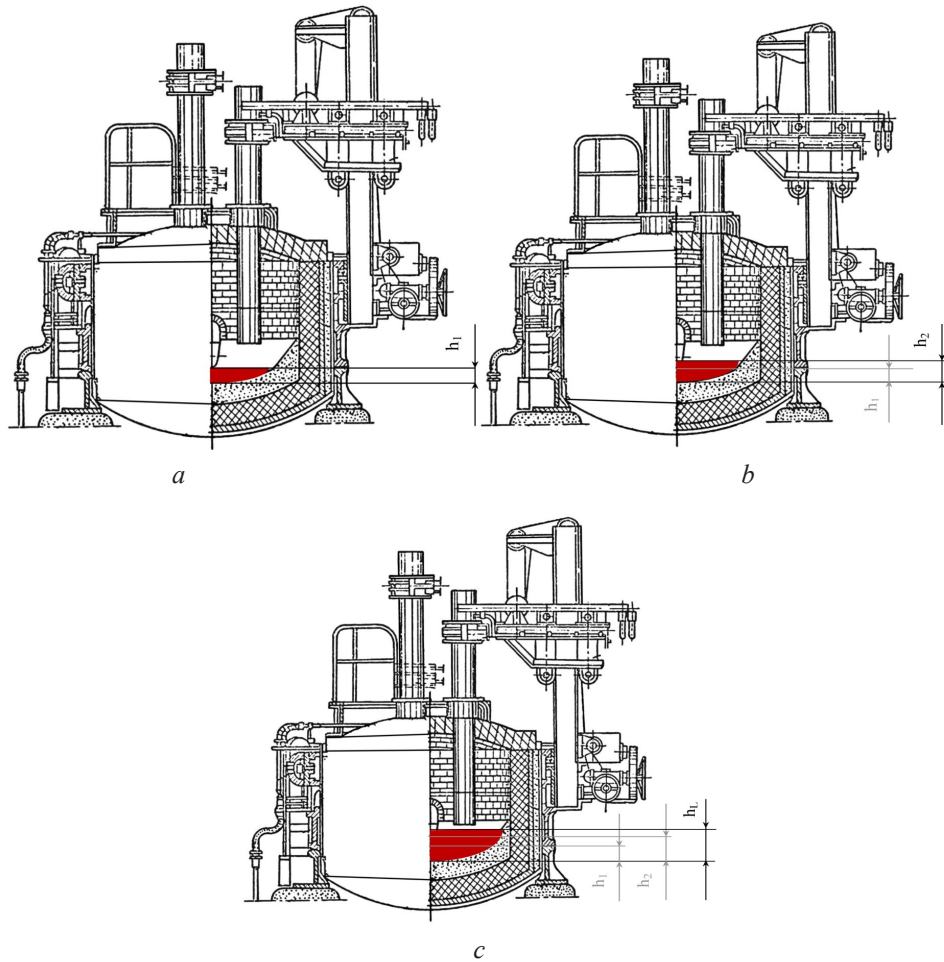


**Fig. 14.** Filling the mixer with portions of the melt dispensed from the cupola at moments  $j (j=1, \dots, L)$  [9]:  $a - j=1 \rightarrow h=h_1$ ;  $b - j=2 \rightarrow h=h_2$ ;  $c - j=L \rightarrow h=h_L, j$  – time point of the melt dispensing from the cupola into the mixer;  $h_j$  – depth of the bath in the mixer when melt is discharged with a volume of  $V_i$  from the cupola

**Table 7**  
 Technical characteristics of the electric furnace

No.	Name	Dimension	Characteristics	Motes
1	Furnace capacity	t	10	cast iron
2	Power transformer	kW	2250	–
3	Transformer low side voltage	V	150 125 105	With deviations $\pm 5\%$
4	Maximum furnace current	A	10400	–
5	Number of phases	–	3	–
6	Current frequency	$s^{-1}$	50	–
7	Electrode diameter	mm	350	–
8	Electrode decay diameter	mm	900	–
9	Electrode stroke	mm	1200	–
10	Electrode speed	m/min	1.65	–
11	Bath diameter at threshold	mm	2350	–
12	Depth of the bath to the threshold	mm	560	–
13	Working window dimensions	mm×mm	780×460	Width×height
14	40° tilt time	S	56	minimal
15	Specific energy consumption for cast iron heating	kW·h/t	105	When heated from 1400 to 1550 °C
16	Cooling water consumption	m <sup>3</sup> /h	15	–
17	The total weight of the furnace metal	T	23.6	–

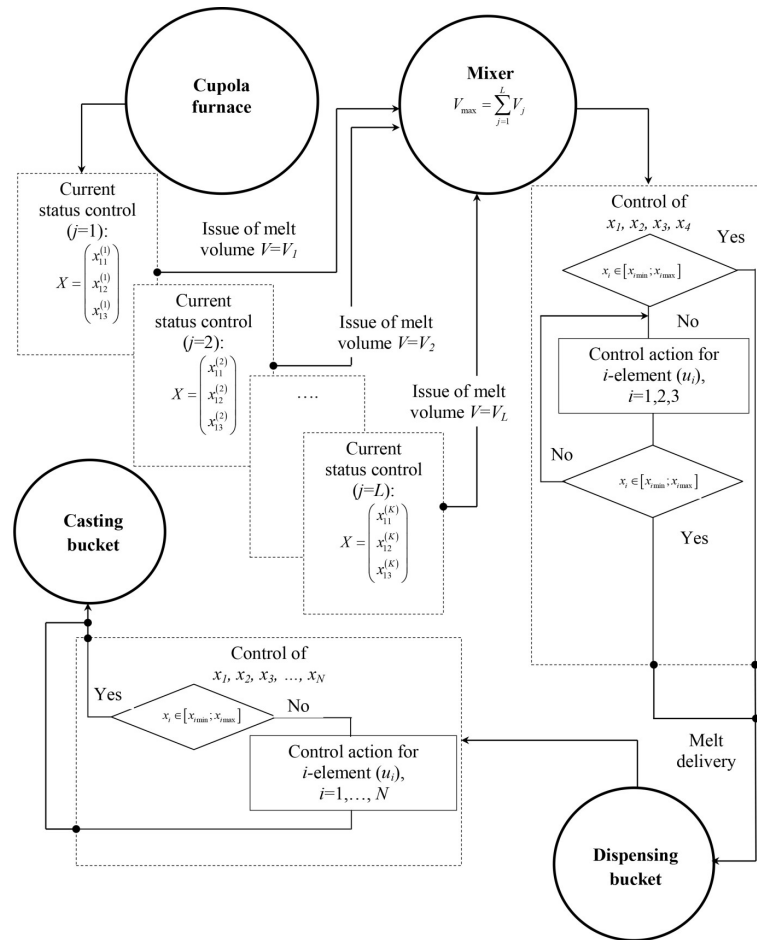


**Fig. 15.** Diagram of the control system of the technological system «cupola – mixer» [9]:  $x_i$  – the content of the  $i$ -th element of chemical composition in cast iron,  $x_{ij}$  – the content of the  $i$ -th element of chemical composition in the  $j$ -th portion of the melt discharged from the cupola into the mixer

**Table 8**

The amount and method of introducing additives to reduce the content of elements in cast iron [9]

Name of additives	The amount of additive, kg per 1 ton of molten iron, introduced into the mixer DChM-10					
	Si, %			Mn, %		Cr, %
Steel scrap	0.1	0.2	0.3	0.1	0.2	0.1
Converted cast iron	12	25	38	42	84	74
–	26	51	76	83	166	148
	In this case, Mn is introduced, %			In this case, Si is introduced, %		In this case, the following shall be introduced: Mn=0.17 %; Si=0.1 %
	0.018	0.038	0.057	0.06	0.12	–

**Table 9**

The amount and method of introducing additives to increase the content of elements in cast iron [9]

Name of additives	The amount of additive, kg per 1 ton of molten iron, introduced into the mixer DChM-10					
	Si, %	Mn, %	Cr, %	C, %	Ti, %	Cu, %
Ferrosilicon FS-25	0.1	0.1	0.1	0.1	0.1	0.1
Ferromanganese FMN-70	4.4	–	–	–	–	–
Ferrochrome	–	1.3*	–	–	–	–
Converted cast iron	–	–	1.85	–	–	–
Titanium copper cast iron	–	–	–	25	–	–
	–	–	–	–	13.3	36.3

Note: \* – given to the bottom of the bucket



**Fig. 16.** Production of top half-forms by additional pressing without rotating the half-forms

There were 3 models on the model plate with additional feeding elements of the gating system provided in order to prevent the formation of porosity.

The finished castings were primed and subjected to quality control for dimensional and geometric accuracy, mechanical properties were checked on standard samples, the chemical composition was controlled after the modification operation at the stage of dispensing cast iron from the mixer before pouring. The microstructure was determined in the factory laboratory. The finished casting is shown in **Fig. 17**.



**Fig. 17.** Casting “clutch release cylinder housing”

To improve the existing technology, a hypothesis was put forward that it is possible to reduce the weight and size characteristics of castings by increasing the tensile strength of cast iron. This would make it possible to make adjustments to the casting equipment in order to, in addition to reducing the weight and size characteristics, provide a resource-saving effect on the finished cast iron. The possibility of increasing the tensile strength at increased carbon content was assumed to be important. It was assumed that this could be achieved by alloying cast iron with a minimum amount of elements that promote the formation of a microstructure with a pearlite matrix with minimal graphite sizes, but without residual  $Fe_3C$ . Therefore, the task was set to optimize the composition of Cr/Ni – Cu/Ti alloying complexes, in which alloying elements were introduced as part of the charge, followed by modification of the cast iron melt with ferrosilicon FeSi75.

**3. Results**

The study was carried out in an industrial environment with the implementation of a passive experiment plan, during which a sample of data from 200 melts was obtained on the chemical compositions and tensile strength of cast iron.

**Fig. 18–20** show diagrams for the content of C, Cr, Cu in cast irons of serial melts, and in **Fig. 21** – tensile strength values.

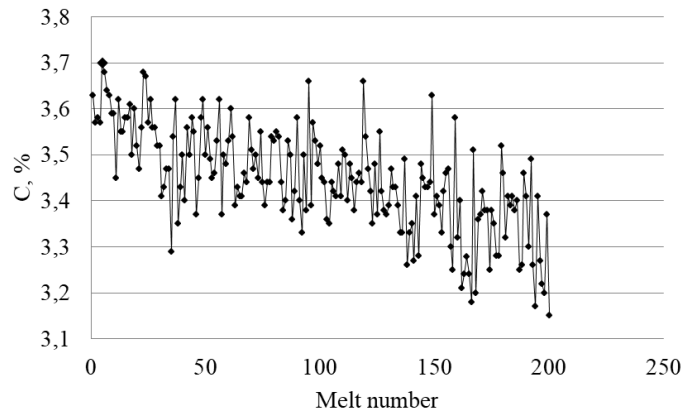


**Fig. 18.** Carbon content in cast irons of serial melts

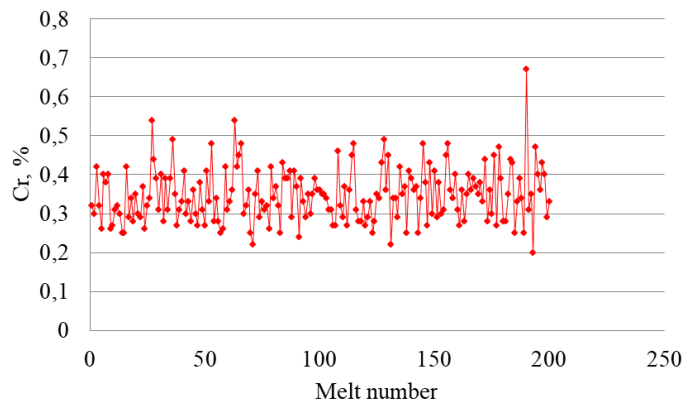


**Fig. 19.** Chromium content in cast irons of serial melts

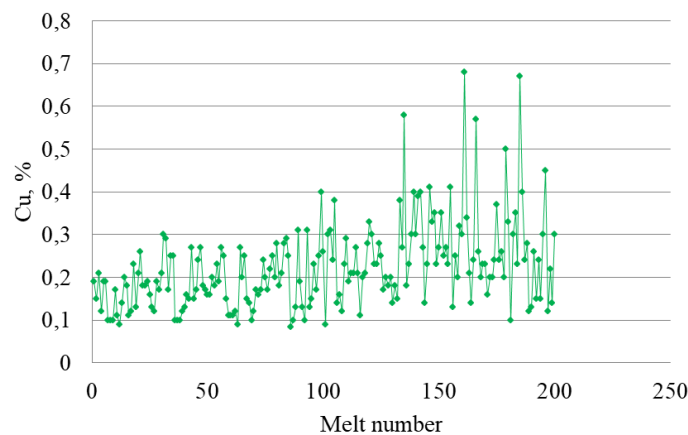


**Fig. 20.** Copper content in cast irons of serial melts

From the total data sample, 25 lines were selected with the results of melts corresponding to the cast iron grades EN-GJL-250 and EN-GJL-300 with an average tensile strength of 270 MPa.



For these lines, a mathematical model  $C=f(\text{Cr}, \text{Cu})$  was built, which has the form of a regression equation. Thus, it was necessary to find the ratio of the content of graphitizing and carbide-forming elements of the chemical composition that form an equal value of the tensile strength. The geometric interpretation of this problem is as follows: find the section of the response surface  $\sigma_b=\varphi(\text{C}, \text{Cr}, \text{Cu})$  in the factor space of input variables formed by the content of C, Cr, Cu, the plane  $\sigma_b=270$  MPa and, based on this section of the response surface, obtain  $C=f(\text{Cr}, \text{Cu})$ . The general form of the equation  $\sigma_b=\varphi(\text{C}, \text{Cr}, \text{Cu})$  is a second-degree polynomial that describes the output variable in a three-dimensional factor space [30]. Based on the study of the final response surface  $C=f(\text{Cr}, \text{Cu})$ , the optimal compositions of alloying complexes Cr – Cu were found, providing a given level of tensile strength with the maximum possible carbon content in cast iron. Since in the technological process under study Ni is contained in the same charge material as Cr, and Ti in the same charge material as Cu, it is possible to talk about a Cr/Ni – Cu/Ti alloying complex.

General form of the equation describing the response surface  $C=f(\text{Cr}, \text{Cu})$ :

$$y = a_0 + 2\mathbf{a}^T \mathbf{x} + \mathbf{x}^T \mathbf{A} \mathbf{x}, \tag{8}$$

where  $y$  – the tensile strength value ( $\sigma_b$ );

$\mathbf{x}$  – matrix of input variables with components  $x_1$  (input variable – Cr), and  $x_2$  (input variable – Cu), in normalized form;

$\mathbf{x}^T$  – transposed matrix of input variables;

$a_0$  – the initial term of the regression equation;

$\mathbf{a}^T$  – transposed matrix of linear terms of the regression equation;

$\mathbf{A}$  – matrix of nonlinear coefficients of the regression equation.

The normalized values of the input variables were determined by the formula:

$$x_i = \frac{2x_{in} - (x_{in\max} + x_{in\min})}{x_{in\max} - x_{in\min}}, \quad i = 1, 2, \dots, N, \tag{9}$$

where  $x_{in\max}$  – the maximum value of the  $i$ -th input variable in the selected range of variation in natural form;

$x_{in\min}$  – the minimum value of the  $i$ -th input variable in the selected range of variation in natural form;

$x_{in}$  – the value of the  $i$ -th input variable in natural form;

$x_i$  – the value of the  $i$ -th input variable in normalized form.

Conversion of normalized values into natural ones was carried out according to the formula

$$x_{in} = x_i I_i + \bar{x}_i, \tag{10}$$

where  $\bar{x}_i$  – the average values of the input variables,  $I_i$  – the intervals of variation of the input variables  $I_i = x_{in\max} - x_{in\min} = x_i - x_i^{\min}$ .

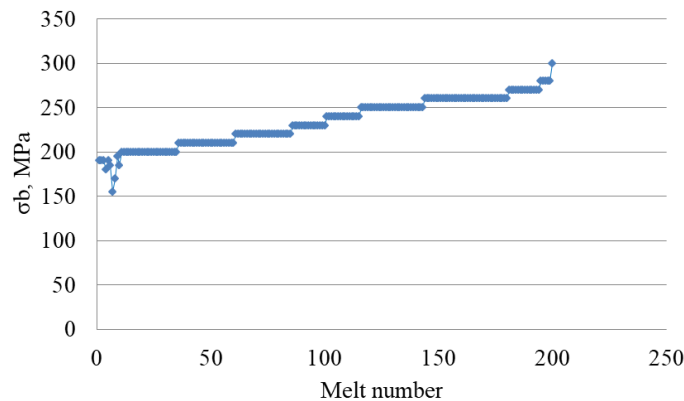


Fig. 21. Tensile strength of cast iron of serial melts

The following intervals of variation of input variables are accepted: Cr=(0.2–0.67) %, Cu=(0.1–0.67) %. The average ratio of alloying elements Cr/Ni and Cu/Ti corresponded to: Cr/Ni=1.75, Cu/Ti=4.8.

The coefficients of equation (8) were determined by the least squares method:

$$\mathbf{A} = (\mathbf{F}^T \mathbf{F})^{-1} \mathbf{F}^T \mathbf{Y} = \mathbf{C} \mathbf{F}^T \mathbf{Y}. \tag{11}$$

where  $\mathbf{F}$  – the matrix of the experimental plan,  $\mathbf{F}^T$  – the transposed matrix of the experimental plan,  $\mathbf{A}$  – the matrix of estimates of the coefficients of the regression equation,  $\mathbf{Y}$  – the matrix of values of the output variable ( $S$ ),  $\mathbf{C}$  – the dispersion matrix.

**Table 10** shows the calculated values of the equation coefficients, presented in matrix form.

**Table 10**  
Coefficient estimation matrices

$a_0$	$\mathbf{a}$	$\mathbf{A}$
3.3069	$\begin{pmatrix} -0.06465 \\ -0.04385 \end{pmatrix}$	$\begin{pmatrix} 0.1148 & -0.1163 \\ -0.1163 & -0.1542 \end{pmatrix}$

The method of steep ascent along the response surface [31] was not used, since it was not possible to conduct an active experiment under the conditions of existing mass production. The response surface analysis was carried out on the basis of its canonical transformation [18, 19] and ridge analysis [32–34], which makes it possible to find optimal values of input variables taking into account the restrictions imposed by the area of experiment planning.

As a result of the canonical transformation, the response surface was reduced to the form:

$$y - y^* = \lambda_1 \xi_1^2 + \lambda_2 \xi_2^2, \tag{12}$$

where  $\lambda_1, \lambda_2$  – the eigenvalues of matrix  $\mathbf{A}$  (Table 5),  $\lambda_1 = -0.1975, \lambda_2 = 0.1581, \xi_1, \xi_2$  – coordinates obtained by rotating the  $x_1$  and  $x_2$  axes during the canonical transformation,  $y^* = 3.34$  %.

Thus, the equation describing the response surface  $C=f(\text{Cr}, \text{Cu})$  has the following canonical form:

$$y - 3.34 = -0.19751 \xi_1^2 + 0.158109 \xi_2^2. \tag{13}$$

Based on the fact that  $|\lambda_1| \neq |\lambda_2|, \lambda_1 < 0, \lambda_2 > 0$ , it is concluded that the response surface is a hyperbolic paraboloid. This means that the content of alloying elements ensuring a tensile strength of 270 MPa and higher – up to 300 MPa with increased carbon content – will be on the boundaries of the planning area.

The results of ridge analysis of the response surface, obtained by numerically solving the ridge line equations in parametric form (14), are shown in **Fig. 22–24**.

$$\begin{cases} \mathbf{x}^*(\lambda) = (\lambda \mathbf{I} - \mathbf{A})^{-1} \mathbf{a}, \\ r^*(\lambda) = \sqrt{\mathbf{x}^{*T} \mathbf{x}^*}, \\ y^*(\lambda) = \mathbf{a}_0 + 2\mathbf{a}^T \mathbf{x}^* + \mathbf{x}^{*T} \mathbf{A} \mathbf{x}^*, \end{cases} \tag{14}$$

where  $\mathbf{x}^*(\lambda)$  – the matrix of suboptimal values of input variables in normalized form, depending on the parameter  $\lambda, \mathbf{x}^{*T}(\lambda)$  – the transposed matrix of suboptimal values of input variables,  $r^*(\lambda)$  – the radius of a circle limiting the area of input variables,  $\mathbf{I}$  – identity matrix,  $\mathbf{a}_0, \mathbf{a}, \mathbf{A}$  – matrices of coefficient estimates,  $\mathbf{a}^T$  – transposed matrix of coefficient estimates for linear terms.

Based on the results of the ridge analysis presented in **Fig. 22–24**, it is possible to conclude that the optimal solutions are those located on ridge line IV. The optimal values of the input variables corresponding to this line are found from the second equation of the system (14). They form many sets of Cr/Ni – Cu/Ti, which must be introduced into the melt in the form of ferroalloys at the stage of out-of-furnace processing or with the charge directly into the furnace, depending on the carbon content in the

melt at the time of release of the cast iron from the furnace. Such sets provide the production of cast iron with a tensile strength of 270–300 MPa, that is, a transition from cast iron grade EN-GJL-200 to grades EN-GJL-250 and EN-GJL-300. The choice of specific options is carried out for reasons of minimizing the cost of charge materials and is recorded in the regulatory documents for melt.

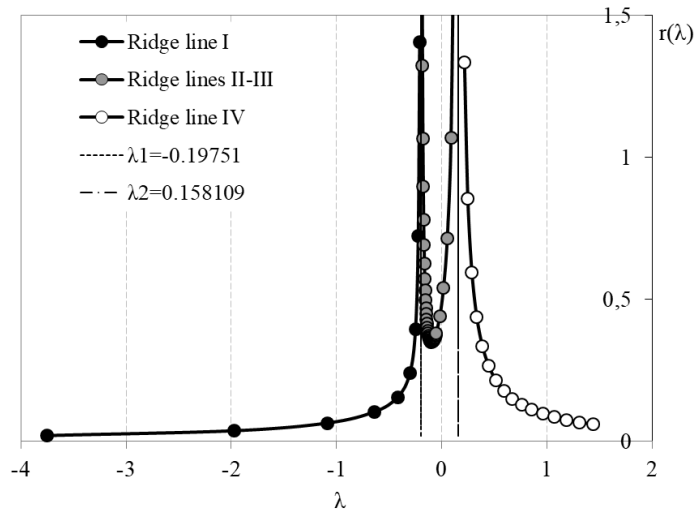


Fig. 22. Parametric dependence  $r=r(\lambda)$

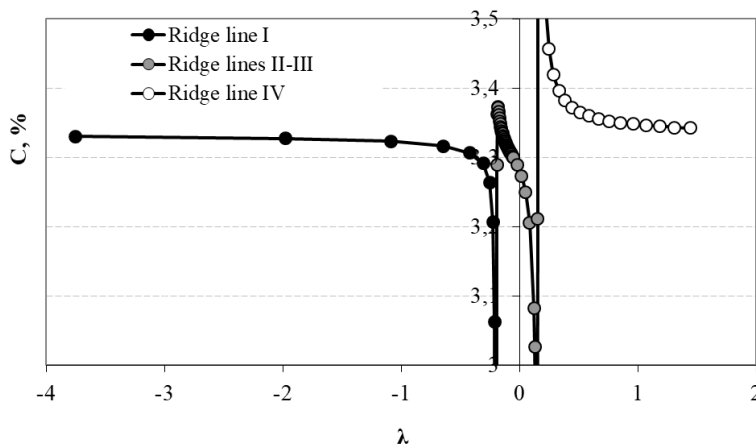


Fig. 23. Parametric dependence  $C=C(\lambda)$

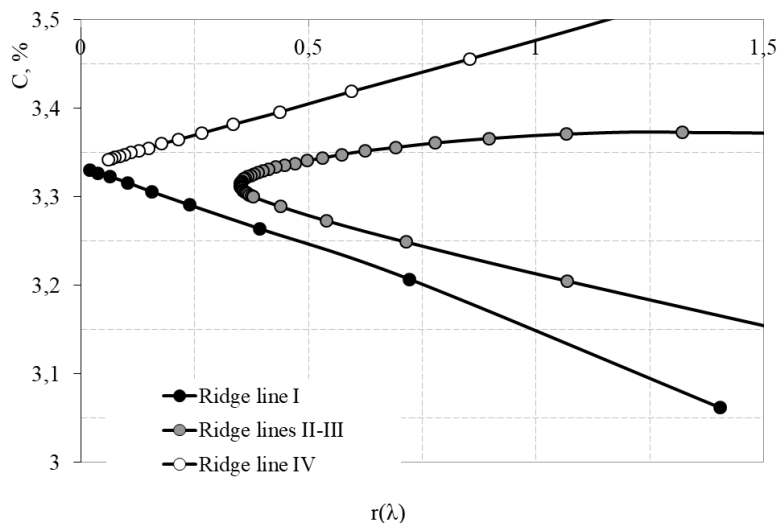


Fig. 24. Parametric dependence  $C=C(r)$

In the study, out of many optimal solutions, one was selected for calculating the charge; the chemical composition and quantity of charge components is the commercial information of the enterprise. The regulations for the production of cast iron, built on the basis of the selected optimal option for melt cast iron for castings of a “clutch release body” of a specific brand of truck, ensured the production of a pearlite structure with a minimum size of graphite and the absence of cementite.

Fig. 25, 26 show histograms of graphite size distribution on the surface of the sample and in the axial zone of the sample.

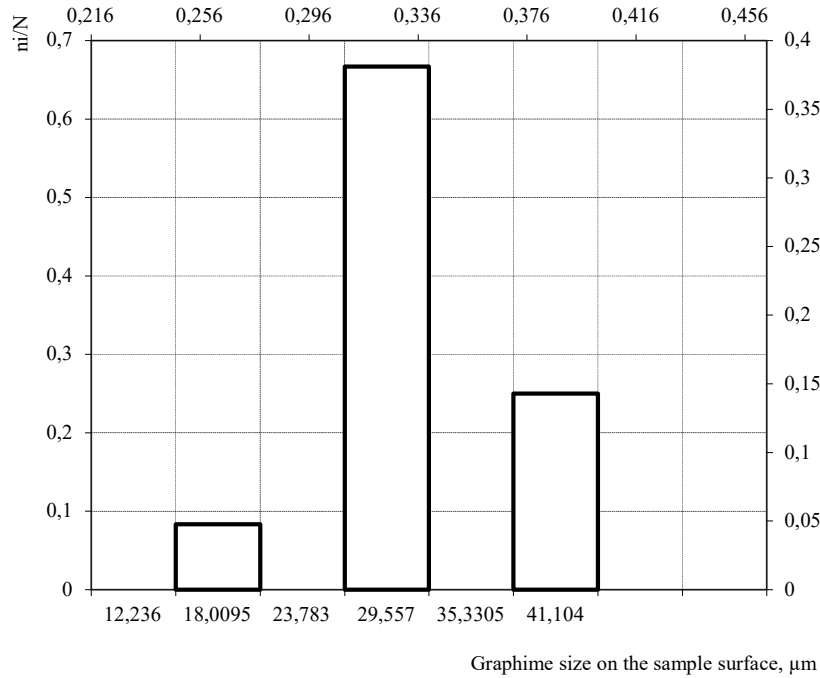


Fig. 25. Histogram of graphite size distribution on the sample surface:  $M(x)=26.15 \mu\text{m}$ ,  $s=5.83 \mu\text{m}$

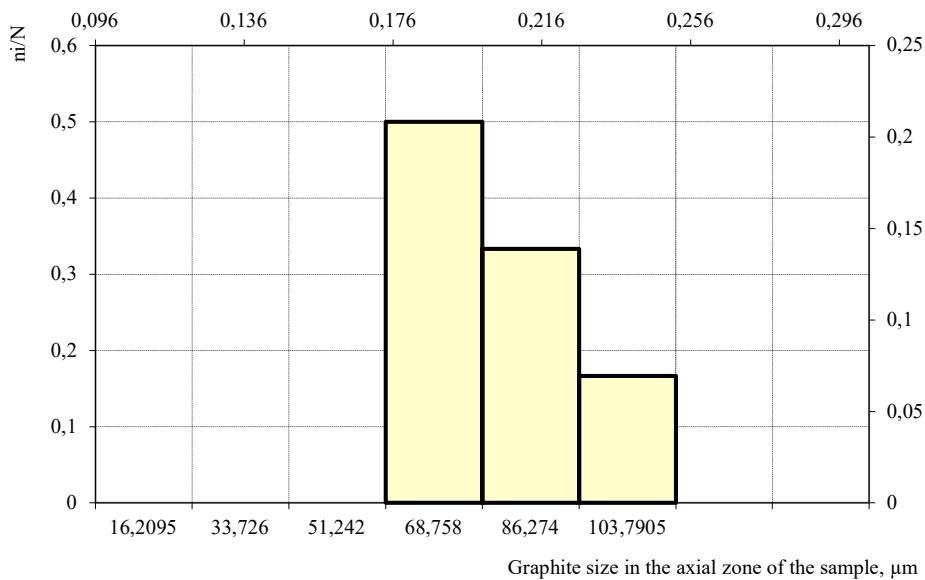
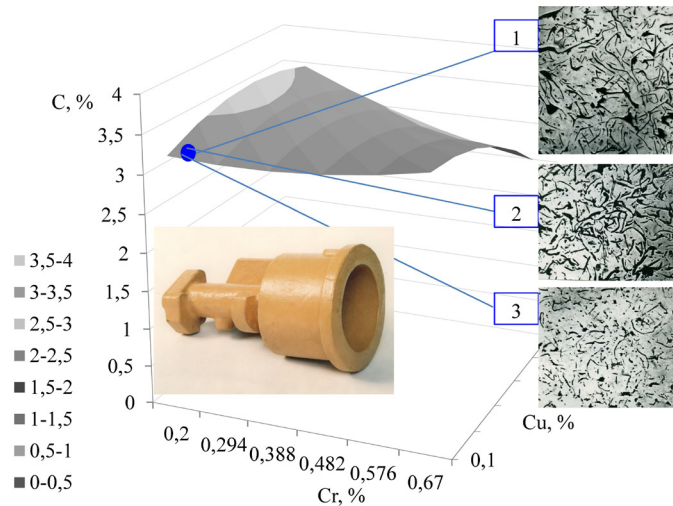


Fig. 26. Histogram of graphite size distribution in the axial zone of the sample:  
 $M(x)=58.85 \mu\text{m}$ ,  $s=17.28 \mu\text{m}$

In Fig. 25, 26 the following notations are used:  $M(x)$  – the mathematical expectation of the graphite size,  $s$  – the standard deviation of the graphite size.

In all cases, the metal matrix included 96–100 % pearlite. This microstructure ensured the required tightness of the castings. However, it should be noted that due to the loss of survivability of the modifier at the stage from the release of the melt from the mixer, which is preceded by the modification procedure, to the filling of the last mold, the dimensions and distribution of graphite change, and the properties of cast iron change accordingly. **Fig. 27** shows the response surface and photographs of microstructures observed within 15 minutes from the moment of introducing the modifier to the filling of the last mold. The capacity of the transfer ladle was 2 tons, the capacity of the casting ladles was 0.5 tons.



**Fig. 27.** Visualization of the response surface and loss of survivability of the modifier, affecting changes in the size and distribution of graphite: 1 – time interval from the moment of modification 5 minutes, 2 – time interval from the moment of modification 10 minutes, 3 – time interval from the moment of modification 15 minutes; ● – area of chemical composition for which the microstructure was analyzed

Thus, the main improvement in the manufacturing technology of the clutch release cylinder body is the optimization of the technology of melt and after-furnace processing, which is based on the determination of the optimal compositions of alloying Cr/Ni – Cu/Ti complexes (**Fig. 24**). Choosing one of the optimal options makes it possible to increase the grade of cast iron by increasing the tensile strength at higher carbon contents. This can make it possible to reduce the thickness of the walls of castings, achieving a reduction in their weight and size characteristics, making adjustments to the design of casting equipment.

A diagram showing an improved part of the technology for manufacturing the clutch release cylinder housing casting is shown in **Fig. 28**.

The proposed improvement makes it possible to purposefully select melt processing modes that allow increasing the strength characteristics of cast iron for cast body parts, thereby moving from the EN-GJL-200 cast iron grade to the EN-GJL-250 and EN-GJL-300 grades.

The limitations of this study should, however, be noted. The simulation results are limited by the intervals of variation of input variables and, accordingly, by the area of passive experiment planning. This does not allow to talk about the adequacy of the resulting model outside this area. In addition, if to talk about the size and distribution of graphite as the main factors determining tightness, it is necessary to take into account that these parameters are not random variables. Therefore, constructing distribution histograms for the purpose of quantitative estimates of these parameters is not fully justified. This is due to the very method of determining the size of graphite, which is based not on the use of technical measuring instruments, but on expert assessments based on comparison of the observed microstructure with images of the standard. This assessment method is convenient and acceptable for practical conditions, but is inaccurate enough to obtain a high-quality mathematical description that can be used to optimize

technological conditions for melt and after-furnace processing. In this case, the size of graphite should be considered not as a random variable, but as a fuzzy value described by some kind of membership function. In this case, to evaluate it, it is necessary to operate with the concepts of modal meaning and the compactness of the body of uncertainty. Therefore, a possible direction for the development of research in terms of improving the processes of melt and out-of-furnace processing for targeted regulation of the formation of microstructure and properties may be additional research in the area of planning. This is possible by implementing an artificial orthogonalization procedure, which allows one to obtain the most accurate estimates of the coefficients of the “composition-properties” mathematical model, in which the microstructure parameters as output variables can be considered in the form of fuzzy numbers.

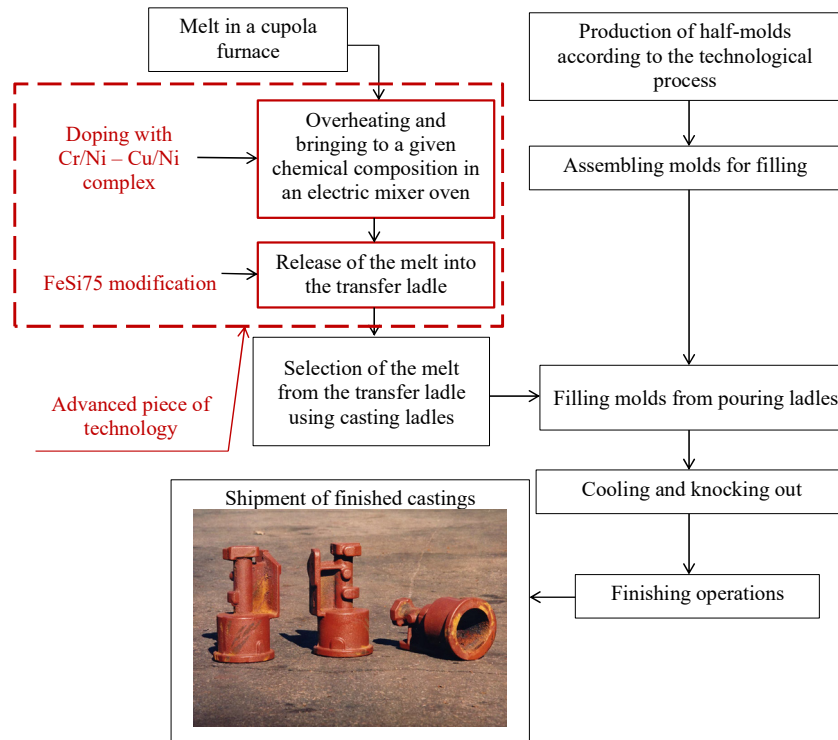


**Fig. 28.** The essence of improving the technology for manufacturing the casting of the clutch release cylinder housing

#### 4. Conclusions

The developed mathematical model in the factor space of independent input variables Cr – Cu and subsequent optimization using this model made it possible to determine the compositions of alloying Cr/Ni – Cu/Ti complexes that ensure an increase in the grade of cast iron by increasing the tensile strength at elevated carbon contents. This makes it possible in the future to reduce the thickness of the walls of the castings, achieving a reduction in their weight and size characteristics.

The technology for manufacturing castings of the clutch release cylinder body, improved in this part, makes it possible to purposefully select melt processing modes, ensuring an increase in the strength characteristics of cast iron for these castings from 200 to 270–300 MPa, thereby moving from the EN-GJL-200 cast iron grade to the EN-GJL-250 and EN-GJL-300 grades.

#### Conflict of interest

The authors declare that there is no conflict of interest in relation to this paper, as well as the published research results, including the financial aspects of conducting the research, obtaining and using its results, as well as any non-financial personal relationships.

#### Funding

The study was performed without financial support.

**Data availability**

Data will be made available on reasonable request.

**Use of artificial intelligence**

The authors confirm that they did not use artificial intelligence technologies when creating the current work.

**References**

- [1] Luis, C. J., Álvarez, L., Ugalde, M. J., Puertas, I. (2002). A technical note cupola efficiency improvement by increasing air blast temperature. *Journal of Materials Processing Technology*, 120 (1-3), 281–289. doi: [https://doi.org/10.1016/s0924-0136\(01\)01053-6](https://doi.org/10.1016/s0924-0136(01)01053-6)
- [2] O'Brien, W. A., Ohio, F. (1948). Pat. No. 2 443 960 USA. Control means for cupola furnaces. United States Patent Office. Serial No. 525,686 5 Claims (Cl. 266–30)
- [3] Isnugroho, K., Birawidha, D. C. (2018). The production of pig iron from crushing plant waste using hot blast cupola. *Alexandria Engineering Journal*, 57 (1), 427–433. doi: <https://doi.org/10.1016/j.aej.2016.11.004>
- [4] Larsen, E. D., Clark, D. E., Moore, K. L., King, P. E. (1997). Intelligent control of Cupola Melting. Available at: <https://pdfs.semanticscholar.org/56c2/96af1d56d5cd963a5bcc38635142e5fa1968.pdf>
- [5] Moore, K. L., Abdelrahman, M. A., Larsen, E., Clark, D., King, P. (1998). Experimental control of a cupola furnace. *Proceedings of the 1998 American Control Conference. ACC (IEEE Cat. No.98CH36207)*. doi: <https://doi.org/10.1109/acc.1998.703360>
- [6] Jezierski, J., Janerka, K. (2011). Selected Aspects of Metallurgical and Foundry Furnace Dust Utilization. *Polish Journal of Environmental Studies*, 20 (1), 101–105.
- [7] Demin, D. (2023). Experimental and industrial method of synthesis of optimal control of the temperature region of cupola melting. *EUREKA: Physics and Engineering*, 2, 68–82. doi: <https://doi.org/10.21303/2461-4262.2023.002804>
- [8] Barinov, N. A., Aleksandrov, N. M. (1969). Vliianie domennykh chugunov v sostave vagranochnykh shikht na kachestvo otlivok massovogo proizvodstva. *Liteinoe proizvodstvo*, 3, 10–11.
- [9] Demin, D. (2019). Development of «whole» evaluation algorithm of the control quality of «cupola – mixer» melting duplex process. *Technology Audit and Production Reserves*, 3 (1 (47)), 4–24. doi: <https://doi.org/10.15587/2312-8372.2019.174449>
- [10] Demin, D. (2020). Constructing the parametric failure function of the temperature control system of induction crucible furnaces. *EUREKA: Physics and Engineering*, 6, 19–32. doi: <https://doi.org/10.21303/2461-4262.2020.001489>
- [11] Stanovska, I., Duhanets, V., Prokopovych, L., Yakhin, S. (2021). Classification rule for determining the temperature regime of induction gray cast iron. *EUREKA: Physics and Engineering*, 1, 60–66. doi: <https://doi.org/10.21303/2461-4262.2021.001604>
- [12] Dymko, I. (2018). Choice of the optimal control strategy for the duplex-process of induction melting of constructional iron. *EUREKA: Physics and Engineering*, 4, 3–13. doi: <https://doi.org/10.21303/2461-4262.2018.00669>
- [13] Trufanov, I. D., Chumakov, K. I., Bondarenko, A. A. (2005). Obshheteoreticheskie aspekty razrabotki stokhasticheskoi sistemy avtomatizirovannoi ekspertnoi otsenki dinamicheskogo kachestva proizvodstvennykh situatsii elektrostaleplavleniia. *Eastern-European Journal of Enterprise Technologies*, 6 (2 (18)), 52–58.
- [14] Trufanov, I. D., Metelskii, V. P., Chumakov, K. I., Lozinskii, O. Iu., Paranchuk, Ia. S. (2008). Energosberegaiushhee upravlenie elektrotekhnologicheskim kompleksom kak baza povysheniia energoeffektivnosti metallurgii stali. *Eastern-European Journal of Enterprise Technologies*, 6 (1 (36)), 22–29.
- [15] Demin, D. A., Pelikh, V. F., Ponomarenko, O. I. (1995). Optimization of the method of adjustment of chemical composition of flake graphite iron. *Liteynoe Proizvodstvo*, 7-8, 42–43.
- [16] Demin, D. A., Koval, O. S., Kostik, V. O. (2013). Technological audit of modifying cast iron for casting automobile and road machinery. *Technology Audit and Production Reserves*, 5 (1 (13)), 58–63. doi: <https://doi.org/10.15587/2312-8372.2013.18398>
- [17] Demin, D. A. (1998). Change in cast iron's chemical composition in inoculation with a Si-V-Mn master alloy. *Litejnoe Proizvodstvo*, 6, 35.
- [18] Demin, D. (2017). Strength analysis of lamellar graphite cast iron in the «carbon (C) – carbon equivalent (Ceq)» factor space in the range of C = (3,425-3,563) % and Ceq = (4,214-4,372) %. *Technology Audit and Production Reserves*, 1(1(33)), 24–32. doi: <https://doi.org/10.15587/2312-8372.2017.93178>
- [19] Demin, D. (2018). Investigation of structural cast iron hardness for castings of automobile industry on the basis of construction and analysis of regression equation in the factor space «carbon (C) – carbon equivalent (Ceq)». *Technology Audit and Production Reserves*, 3 (1 (41)), 29–36. <http://doi.org/10.15587/2312-8372.2018.109097>
- [20] Frolova, L., Shevchenko, R., Shpyh, A., Khoroshailo, V., Antonenko, Y. (2021). Selection of optimal AL-SI combinations in cast iron for castings for engineering purposes. *EUREKA: Physics and Engineering*, 2, 99–107. doi: <https://doi.org/10.21303/2461-4262.2021.001694>
- [21] Frolova, L., Barsuk, A., Nikolaiev, D. (2022). Revealing the significance of the influence of vanadium on the mechanical properties of cast iron for castings for machine-building purpose. *Technology Audit and Production Reserves*, 4 (1 (66)), 6–10. doi: <https://doi.org/10.15587/2706-5448.2022.263428>

- [22] Nikolaiev, D. (2022). Procedure for selecting a rational technological mode for the processing of cast iron melt on the basis of graph-analytical processing of the data of serial smeltings. *ScienceRise*, 5, 3–13. doi: <https://doi.org/10.21303/2313-8416.2022.002774>
- [23] Demin, D. (2017). Synthesis of nomogram for the calculation of suboptimal chemical composition of the structural cast iron on the basis of the parametric description of the ultimate strength response surface. *ScienceRise*, 8, 36–45. doi: <https://doi.org/10.15587/2313-8416.2017.109175>
- [24] Frolova, L. V. (2011). Identification provision of energy saving on the basis of audit process moulding machines shaking. *Technology Audit and Production Reserves*, 2 (2 (2)), 8–13. doi: <https://doi.org/10.15587/2312-8372.2011.4859>
- [25] Frolova, L. V. (2012). Choice of ways to improve design elements of machines moulding shaking. *Technology Audit and Production Reserves*, 1 (1 (3)), 30–34. doi: <https://doi.org/10.15587/2312-8372.2012.4873>
- [26] Lysenkov, V., Demin, D. (2023). Adaptive method of estimating the dynamic characteristics of the bottom pressing process when making disposable casting molds. *Technology Audit and Production Reserves*, 5 (1 (73)), 6–11. doi: <https://doi.org/10.15587/2706-5448.2023.288152>
- [27] Frolova, L. (2023). Search procedure for optimal design and technological solutions to ensure dimensional and geometric accuracy of castings. *Technology Audit and Production Reserves*, 1 (1 (69)), 18–25. doi: <https://doi.org/10.15587/2706-5448.2023.271860>
- [28] Dotsenko, Y., Dotsenko, N., Tkachyna, Y., Fedorenko, V., Tsybul'skyi, Y. (2018). Operation optimization of holding furnaces in special casting shops. *Technology Audit and Production Reserves*, 6 (1 (44)), 18–22. doi: <https://doi.org/10.15587/2312-8372.2018.150585>
- [29] Ivanova, L. A., Prokopovich, I. V. (1997). Vliianie grafitovykh vklucheniin na germetichnost serykh chugunov. *Liteinoe proizvodstvo*, 2, 7–9.
- [30] Kharchenko, S., Barsuk, A., Karimova, N., Nanka, A., Pelypenko, Y., Shevtsov, V., Morozov, I., Morozov, V. (2021). Mathematical model of the mechanical properties of Ti-alloyed hypoeutectic cast iron for mixer blades. *EUREKA: Physics and Engineering*, 3, 99–110. doi: <https://doi.org/10.21303/2461-4262.2021.001830>
- [31] Kuryn, M. (2011). Determination of optimum performance liquid glass of magnetization mixtures with liquid glass. *Technology Audit and Production Reserves*, 2 (2 (2)), 14–20. doi: <https://doi.org/10.15587/2312-8372.2011.4860>
- [32] Kuryn, M. (2012). Synthesis of cold-hardening mixtures with given set of properties and optimization of technological regimes of their manufacturing. *Technology Audit and Production Reserves*, 1 (1 (3)), 25–29. doi: <https://doi.org/10.15587/2312-8372.2012.4872>
- [33] Chibichik, O., Sil'chenko, K., Zemliachenko, D., Korchaka, I., Makarenko, D. (2017). Investigation of the response surface describing the mathematical model of the effects of the Al/Mg rate and temperature on the Al-Mg alloy castability. *ScienceRise*, 5 (2), 42–45. doi: <https://doi.org/10.15587/2313-8416.2017.101923>
- [34] Makarenko, D. (2017). Investigation of the response surfaces describing the mathematical model of the influence of temperature and BeO content in the composite materials on the yield and ultimate strength. *Technology Audit and Production Reserves*, 3 (3 (35)), 13–17. doi: <https://doi.org/10.15587/2312-8372.2017.104895>